ELSEVIER

Chemical Geology 207 (2004) 31–45

CHEMICAL GEOLOGY
INCLUDING
ISOTOPE GEOSCIENCE

www.elsevier.com/locate/chemgeo

The precipitation of aragonite from shallow-water hydrothermal fluids in a coral reef, Tutum Bay, Ambitle Island, Papua New Guinea

Thomas Pichler[a,*], Jan Veizer[b,c]

[a] *Department of Geology, University of South Florida, Tampa, FL 33620, USA*
[b] *Ottawa-Carleton Geoscience Centre, University of Ottawa, Ottawa, Ontario, Canada K1N 6N5*
[c] *Institut fuer Geologie, Mineralogie und Geophysik, 44780 Bochum, Germany*

Received 22 July 2003; accepted 2 February 2004

Abstract

The fringing reef in Tutum Bay on the west side of Ambitle Island, Papua New Guinea is the only presently known coral reef exposed to the extensive discharge of a hot, mineralized hydrothermal fluid. There, aragonite and ferrihydrite, a hydrous ferric oxide, are the prominent hydrothermal precipitates. Aragonite forms two distinct crystal habits, (a) euhedral (pseudo-hexagonal) crystals up to 2 cm long and (b) micro-crystals similar in appearance to ''feather dendrite''. Aragonite encrusts dead coral fragments, volcaniclastic boulders and pebbles, and fills secondary fracture and remaining primary intergranular porosity within volcaniclastic arenite. The hydrothermal aragonite has a distinctively different isotopic composition when compared to ''normal'' shallow-water marine inorganic and organic carbonate that precipitated from seawater. This difference arises from precipitation at high temperature from a mixture of seawater and hydrothermal fluid that has lower $^{87}Sr/^{86}Sr$ and $\delta^{18}O$ values than seawater. Based on a $^{87}Sr/^{86}Sr$ mixing model, aragonite precipitated from a hydrothermal fluid–seawater mixture of approximately 9:1. Precipitation from the hydrothermal solution is mainly caused by CO_2 degassing, but mixing between hydrothermal fluid and seawater may have enhanced precipitation due to an increase in pH.

The $\delta^{13}C$ of Tutum Bay hydrothermal aragonite ranges from 1.9‰ to 2.2‰ (VPDB). This range of values is in good agreement with experimental data [J. Phys. Chem. 72 (1968) 800; Geochim. Cosmochim. Acta 61 (1997) 3461], indicating that C-13-equilibirum has been reached during its formation. Values for $\delta^{18}O$ range from 14.2‰ to 14.7‰ and calculated isotopic equilibrium temperatures are approximately 20 °C lower than directly measured vent fluids and those temperatures obtained from fluid inclusion experiments and the $^{87}Sr/^{86}Sr$ mixing model. This indicates that either oxygen isotope equilibrium was not attained or that the calcite–water fractionation factor for oxygen isotopes is not applicable for the precipitation of Tutum Bay hydrothermal aragonite.

Trace element concentrations, except for the REEs, Y and Sr are low. The REE patterns of aragonite are similar to those of Tutum Bay vent water, indicating the hydrothermal origin of the aragonite. Rare earth element concentrations are higher in the coarse than in the fine-grained aragonite, which might be caused by a change in precipitation rate and seawater mixing.

Keywords: Aragonite; Isotopic equilibrium; Coral reef; Hydrothermal; Seawater; Shallow-water

* Corresponding author.
E-mail address: pichler@chuma.cas.usf.edu (T. Pichler).

0009-2541/$ - see front matter © 2004 Elsevier B.V. All rights reserved.
doi:10.1016/j.chemgeo.2004.02.002

1. Introduction

Previous research on sea floor hydrothermal activity has focused primarily on deep-sea, polymetallic sulfides found along volcanically active portions of the mid-ocean ridges or in deep back-arc basins. There is, however, not much known about either hydrothermal venting or its petrologic definition within shallow-water (nearshore or shallow shelf) carbonate settings associated with volcanic islands.

Throughout the geological record, several occurrences of carbonate minerals have been reported from sedimentary sequences whose precipitation was inferred to be from hydrothermally modified meteoric waters (e.g., Desrochers and Al-Aasm, 1993) or due to venting of cold and/or hot methane rich fluids (e.g., Hovland, 1990; Kaufman et al., 1996). The fringing reef on the west side of Ambitle Island is the only known present-day location where purely hydrothermally driven carbonate deposition is extensively co-occurring with a natural biogenic calcifying community and the formation of mixed carbonate volcaniclastic marine sediments (Pichler and Dix, 1996). Hydrothermal fluids affect adjacent scleractinian corals (Pichler et al., 2000) and the local benthic foraminifera population (Switzer, 1997).

This paper is a continuation of the reconnaissance study by Pichler and Dix (1996) and investigates in detail the precipitation of aragonite from the Tutum Bay hydrothermal fluids. The study of Tutum Bay aragonite provides us with new insights into their precipitation from hydrothermal fluids. We believe that this work is of importance to geologists working in ancient and recent carbonate sediments. It strengthens the conclusion of several studies that interpreted ''unusual'' isotope signatures of paleo-carbonate minerals as being of hydrothermal origin (e.g., Desrochers and Al-Aasm, 1993; Kaufmann and Wendt, 2000). We also demonstrate the possible range of isotopic values found in aragonite on a hand sample scale and provide isotopic considerations for the interpretation of ''unusual'' carbonates. Variations in ancient samples have been used to infer different tectonic settings, whereas our samples have formed in a restricted environment and isotope variations reflect spatial and temporal differences.

2. Description of study area and aragonite deposits

The study area lies along the southwest margin of Ambitle Island, one of the Feni islands in the southernmost island group of the Tabar–Feni chain (Fig. 1). The island is part of a Quaternary stratovolcano with a central eroded caldera built on poorly exposed Oligocene marine limestone (Wallace et al., 1983). Volcanic strata (interbedded lava flows, lahar deposits, tuffs, and scoriae) dip radially from the island, presumably extending beneath the shelf. Several geothermal areas are located primarily along the western coast and in the western part of the caldera near breaches in the caldera wall (Fig. 1). Hot mud pools, springs of chloride and acid sulfate waters, and a few low temperature fumaroles are present, with temperature and pH values ranging from 67 to 100 °C and 1.9 to 9.1, respectively (Licence et al., 1987; Wallace et al., 1983).

Submarine hydrothermal venting occurs at Tutum Bay (Fig. 1) in shallow (5–10 m) water along the inner shelf that contains a patchy distribution of coral–algal reefs surrounded by medium to coarse-grained mixed carbonate-volcaniclastic sand and gravel (Pichler and Dix, 1996). Two types of venting are observed. (1) Focused discharge of a clear, hydrothermal fluid occurs at discrete ports, 10–15 cm in diameter. Fluid temperatures at vent orifices are between 89 and 98 °C. (2) Dispersed or diffuse discharge consists of streams of gas bubbles (94–98% CO_2) emerging directly through the sandy to pebbly unconsolidated sediment and through fractures in volcanic rocks. The hydrothermal fluids are of meteoric origin and possess a salinity (TDS) of approximately 3.5‰ (Pichler et al., 1999). A summary of fluid compositions is presented in Table 1. A more detailed description of Tutum Bay has been provided elsewhere (Pichler et al., 2000, 1999) and color images can be found at http://www.chuma.cas.usf.edu/~pichler.

The precipitation of hydrothermal aragonite in Tutum Bay is not restricted to, but mainly occurs in the immediate (<1 m) vicinity of vent sites. Throughout the bay, hydrothermal fluids seep slowly through the seafloor and cause minor precipitation of aragonite in intergranular spaces in the bottom sediment or in open spaces in the skeletons of dead corals. The bulk precipitation of hydrother-

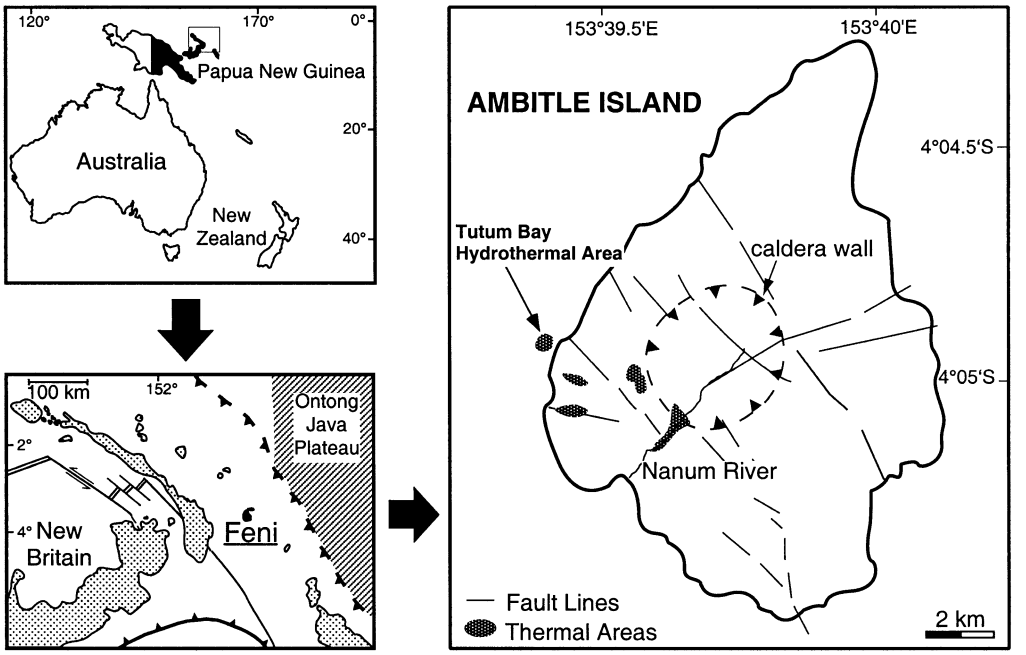

Fig. 1. Location of Ambitle Island, one of the Feni islands in eastern Papua New Guinea (modified after Licence et al., 1987; Pichler and Dix, 1996). Geothermal areas indicated in dark are primarily along the western side of the island.

mal aragonite, however, is in the immediate proximity of the four vent sites, where we collected the samples for this study. A complete listing of all aragonite samples and short description and their location is presented in Table 2.

Aragonite forms isopachous rims, massive monomineralic layers and splays of euhedral (pseudohexagonal) crystals that encrust dead corals and volcaniclastic boulders and pebbles (Fig. 2). Near vent sites, primary pore space in volcaniclastic sediment and in skeletons of dead corals is almost completely occluded by hydrothermal aragonite (Fig. 2b). The growth direction of individual crystals is parallel to each other and normal to their substrate and they can be up to 2 cm long. Larger (coarse) aragonite crystals are generally terminated by scalloped surfaces that do not represent the internal structure and by an abrupt change of crystal habit and size (Fig. 3). Once the growth of coarse crystals ceased the precipitation of much smaller aragonite crystals commenced, growing approximately normal to the surface of the coarse aragonite (Fig. 3b). This later generation of crystals although similar in appearance to "feather-dentritic aragonite", is simply microcrystalline. The black layer immediately adjacent to the coarse aragonite represents a fluid inclusion rich zone (Fig. 3b). The coarse, pointed aragonite crystals in Fig. 3b appear to be made of a random mosaic of anhedral spar crystals that could indicate the inversion of aragonite to calcite. This sparry appearance, however, is an artifact of sample preparation (R. Folk, pers. comm.), because extinction when observed in crossed nicols is uniform (single-crystal extinction).

3. Analytical methods

Hand specimens, polished thin and thick sections were examined using standard light microscopy and scanning electron microscope (SEM) analysis. Mineral identification was confirmed by powder and single-crystal X-ray diffractometry (XRD).

Table 1
Average chemical and isotopic endmember[a] compositions of Tutum Bay hydrothermal fluids compared to seawater (Pichler, 1998, 2003)

Element	Unit	Vents 1–3	Vent 4	Seawater
pH		6.1	6.3	8.03
Cl	ppm	295	357	19,520
Br	ppm	6.8	10.7	45
SO_4	ppm	930	880	2748
HCO_3^-	ppm	840	865	154
B	ppm	8.4	8.6	4.1
Si	ppm	108	105	0.2
Na	ppm	650	665	10,450
K	ppm	76	94	354
Ca	ppm	201	180	405
Mg	ppm	0[a]	0[a]	1235
Li	ppb	1020	990	136
Mn	ppb	495	380	1.6
Fe	ppb	1720	1060	15
Rb	ppb	350	360	104
Sr	ppb	6790	6240	7990
$^{87}Sr/^{86}Sr$	ratio	0.70392	0.70395	0.70918
$\delta^{18}O_{VSMOW}$	‰	−5.1	−5.1	0.4
δD_{VSMOW}	‰	−30.9	−30.2	6.6

[a] Endmember compositions were extrapolated assuming a zero-Mg hydrothermal fluid.

Proton microprobe analyses of polished thin sections were carried out on the Ruhr University, Bochum micro-PIXE, on 20 spots of approximately 5 μm diameter, using a 3 MeV beam (Bruhn et al., 1995) and element concentrations were evaluated with the GUPIX software package (Maxwell et al., 1995). The concentration of elements other than Ca, Mg, Sr, Fe, Mn, and Zn are generally minor in aragonite (e.g., Veizer, 1983) and, therefore, below the detection limit of conventional microbeam methods. Thus, to obtain a more detailed chemical and isotopic composition of the hydrothermal aragonite, the samples V-2D, V-2E, V-3A, V-4.1A and V-4.2B were mechanically separated from coral and volcanic material (e.g., Fig. 2) and powdered in a tungsten-carbide mill. For these samples, major elements were obtained by X-ray fluorescence (XRF) and wet chemical methods. As, Au, Br, Hg, Sb, Se and W were determined by neutron activation analyses (NAA). Ag, Cd, Cs, Hf, In, Mo, Nb, Pb, Rb, Ta, Th, Tl, U, Y, and Zr were determined by inductively coupled plasma mass spectrometry (ICP-MS) and Ba, Be, Co, Cr, Cu, Ni, Sc, Sr, and V were determined by inductively coupled plasma emission spectrometry (ICP-ES). XRD, XRF, SEM, ICP and microprobe analyses were carried out at the Geological Survey of Canada following Hall (1992) and NAA was performed by Activation Labs in Ancaster, Ontario. Analytical errors are as follows: < 2% for

Table 2
Description of Tutum Bay hydrothermal aragonite precipitates

Sample	Year	Location	Description
V-1A	1996	Vent 1	white micritic carbonate matrix in open spaces between volcanic sediment
V-2D	1996	Vent 2	hydrothermal carbonate big clear crystals (Fig. 3) from massive layers in the vent orifice
V-2E	1996	Vent 2	hydrothermal carbonate small white crystal ends on top of V-2D (Fig. 3)
V-3A	1996	Vent 3	white micritic hydrothermal carbonate matrix with some bigger euhedral crystals where space available
FV-3B	1994	Vent 3	dead coral fragment
V-4.1A	1996	Vent 4	white micritic hydrothermal carbonate on top of bigger crystals and below Fe-oxyhydroxides (Fig. 2)
V-4.1B	1996	Vent 4	big clear/gray euhedral aragonite crystals (Fig. 2)
V-4.2A	1996	Vent 4	big clear/gray euhedral aragonite crystals
V-4.2B	1996	Vent 4	fine grained carbonate crust on top of V-4.2A
V-4.3	1996	Vent 4	alternating layers of coarse and fine grained aragonite
FV-4A	1994	Vent 4	big (up to 2 cm) clear/gray euhedral aragonite crystals
FV-4B	1994	Vent 4	fine grained portion of FV-4A
V-2(x)	1996	Vent 2	micro-drilled sample of coarse aragonite from sample V-2 (Fig. 3)
V-2(m)	1996	Vent 2	micro-drilled sample of fine grained (micritic) aragonite from sample V-2 (Fig. 3)
V-4.1(x)	1996	Vent 4	micro-drilled sample of coarse aragonite from sample V-4.1 (Fig. 2)
V-4.1(m)	1996	Vent 4	micro-drilled sample of fine grained (micritic) aragonite from sample V-4.1 (Fig. 2)
V-4.3(x)	1996	Vent 4	micro-drilled sample of coarse aragonite from sample V-4.3
V-4.3(x)	1996	Vent 4	micro-drilled sample of fine grained (micritic) aragonite from sample V-4.3

A map of vent location can be found in Pichler et al. (2000, Fig. 2).

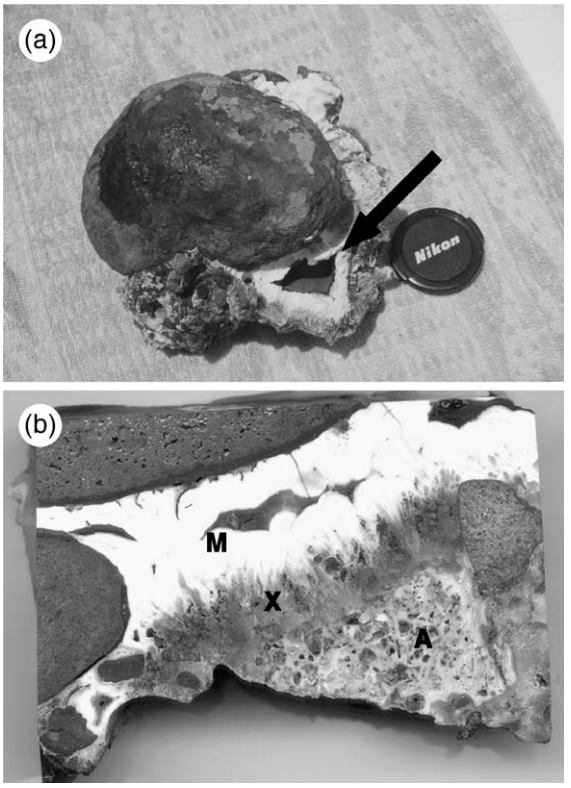

Fig. 2. Petrography of hydrothermal precipitates. (a) Photograph of a large volcanic boulder embedded in a matrix of volcaniclastic sediment, Fe-oxyhydroxide, biogenic carbonate and hydrothermal aragonite. The Fe-oxyhydroxide lined opening on the lower right (arrow) used to be a channel for the hydrothermal fluid. (b) Photograph of a slab from the above hand specimen. This sample clearly shows the change from coral aragonite (A) to euhedral hydrothermal aragonite (X) and then to fine-grained hydrothermal aragonite (M). Field of view is approximately 6 cm.

XRF, < 5% for wet chemical analyses, < 5% for ICP-ES (except < 10% for Ag, Ba and Sr), < 10% for ICP-MS and ~20% for INAA.

Carbon and oxygen isotope analyses of powdered bulk aragonite were performed at the G. G. Hatch Isotope Laboratory, University of Ottawa on a triple collector VG SIRA 12 mass spectrometer. The routine precision was tested using an internal standard and is 0.1‰ for carbon and oxygen. All results are reported in standard delta (δ) notation in per mil (‰) units, relative to the PDB standard for carbon and relative to VSMOW for oxygen, unless otherwise noted. $^{87}Sr/^{86}Sr$ were measured on a five collector Finnigan MAT 262 solid source mass spectrometer at the Institut für Geologie, Ruhr Universität, Bochum following Buhl et al. (1991) and Diener et al. (1996). The average of 100 repeat measurements for the NBS 987 standard was 0.710224 ± 0.000008. Six samples (V-2(x), V-2(m), V-4.1(x), V-4.1(m), V-4.3(x), V-4.3(m)) for O, C and Sr isotope analyses were taken by micro-drilling to allow for a direct comparison between fine

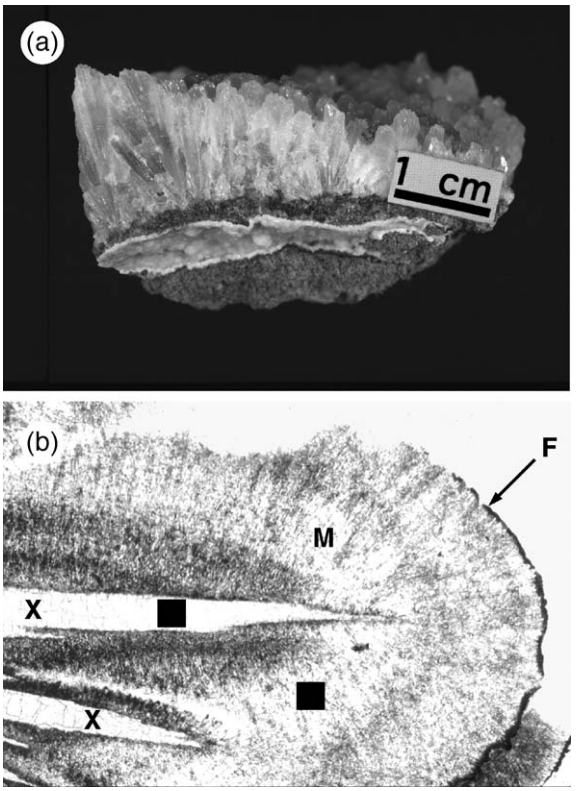

Fig. 3. Petrography of hydrothermal precipitates. (a) Photograph of euhedral, pseudo-hexagonal coarse aragonite from sample V-2. Crystals grow approximately normal to the volcaniclastic substrate. (b) Photograph of a thin section made from sample V-2 showing two pseudo-hexagonal aragonite crystals (X) and radiating micro-crystalline aragonite (M). The micro-crystalline crystals are terminated by a thin layer of Fe-oxyhydroxide (F). The black squares indicate the spots where proton microprobe analyses were performed and where sample material was collected by micro-drilling The sparry appearance of the two pseudo-hexagonal aragonite crystals is an artifact of sample preparation and the black layers are fluid inclusion rich zones. Field of view is approximately 3 mm.

grained and coarse grained aragonite within one sample.

4. Results

4.1. Chemical composition

Despite having precipitated from a hydrothermal fluid, aragonite shows no anomalous concentrations of trace elements and values are similar to "normal" marine abiotic aragonite (e.g., Veizer, 1983). Relative to micro-crystalline aragonite (V-2(m)), coarse aragonite (V-2(x)) is slightly enriched in Ca, Ba, Ga, Pb, Ta and Y, and slightly depleted in Fe, Mn, Rb, Th and Zr (Table 3). The concentration of these elements are close to their respective detection limits. Thus, these values are subject to an increased analytical error and actual differences are likely very small. For Ca, Sr, Fe and Mn, however, the difference could be verified by proton probe analysis (see Fig. 3). Analyses of 10

Table 3
Major, minor and trace element composition of selected Tutum Bay hydrothermal aragonite

Element	Unit	V-2D	V-2E	V-3A	V-4.1A	V-4.2B
SiO_2	%	<0.01	<0.01	<0.5	<0.01	<0.01
TiO_2	%	0.01	<0.02	<0.02	0.01	0.02
Al_2O_3	%	0.10	<0.2	<0.2	0.10	0.34
$Fe_2O_3^T$	%	<0.01	0.07	0.18	<0.01	0.15
MnO	%	<0.01	0.01	0.07	<0.01	0.01
MgO	%	0.05	0.05	0.09	0.04	0.07
CaO	%	53.84	52.60	52.20	53.63	52.00
Na_2O	%	<0.01	0.05	0.05	<0.01	0.08
K_2O	%	<0.01	<0.05	<0.05	<0.01	<0.05
CO_2	%	44.15	44.1	44.0	44.1	n.d.
P_2O_5	%	0.02	0.02	0.02	0.01	<0.01
S^T	%	<0.02	<0.02	<0.02	<0.02	n.d.
Total	%	99.20	97.9	97.9	99.0	53.7
Ag	ppm	0.20	0.2	0.7	0.4	0.1
Ba	ppm	47	<30	<30	<30	<30
Cd	ppm	<0.2	<0.2	<0.2	<0.2	0.4
Cs	ppm	0.04	0.08	0.17	0.05	14
Cu	ppm	<10	<10	<10	<10	18
Ga	ppm	0.7	0.3	1.6	0.3	16
Hf	ppm	0.08	<0.05	0.15	0.12	1.4
Mo	ppm	<0.2	<0.2	<0.2	0.4	3.8
Nb	ppm	0.10	0.10	0.2	0.34	3.0
Pb	ppm	9.5	7	10	10	27
Rb	ppm	0.43	0.76	1.00	0.48	49
Sr	ppm	10,900	11,000	10,000	10,800	9500
Ta	ppm	0.50	<0.2	<0.2	0.8	0.7
Th	ppm	<0.02	0.03	0.1	0.03	0.97
Tl	ppm	0.04	<0.02	<0.02	0.16	0.70
U	ppm	0.03	0.03	0.05	0.05	1.10
Y	ppm	67	24	90	18	47
Zr	ppm	<0.5	0.7	0.9	3.1	49

The following elements, although analyzed, are not listed, because they were below their respective detection limits (in ppm): As (<2), Au (<5), Be (<0.5), Br (<1), Co (<5), Cr (<10), Hg (<1), In (<0.05), Ni (<10), Sb (<0.2), Sc (<0.5), Se (<5), V (<5), W (<4) and Zn (<5).

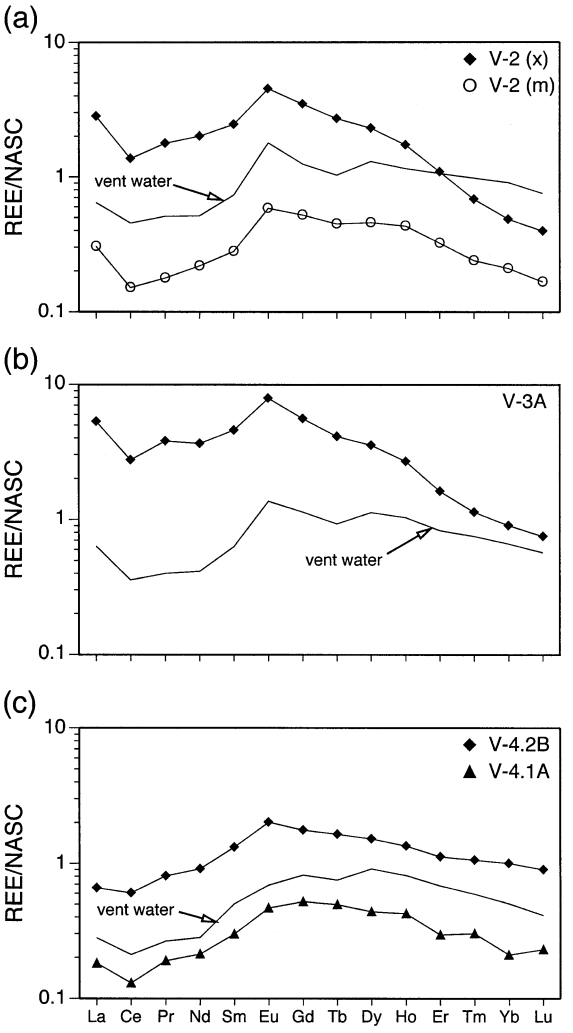

Fig. 4. North American Shale Composite (NASC) (Haskin et al., 1968) normalized rare earth element (REE) plots for hydrothermal aragonite precipitates from vents 2, 3 and 4. Rare earth element concentrations for the respective vent waters are from Pichler et al. (1999) and were multiplied by 10^6.

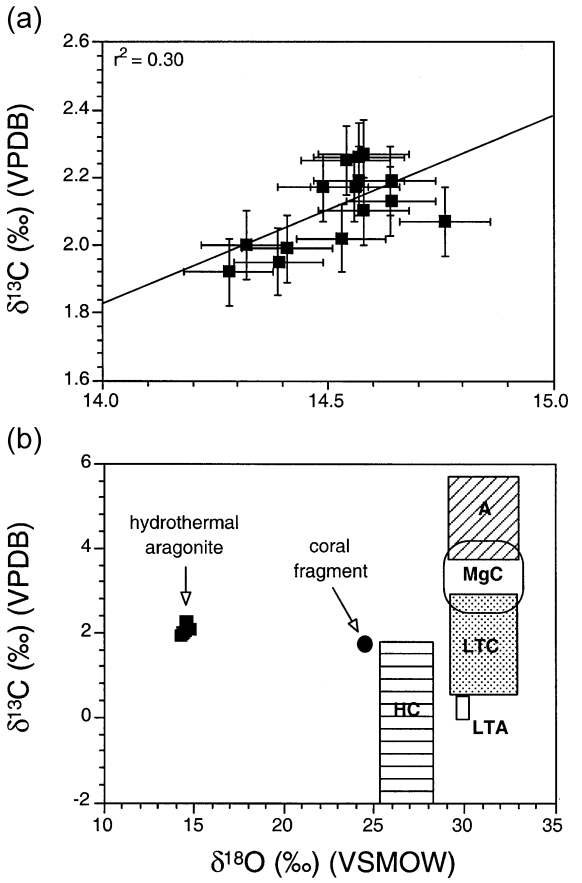

Fig. 5. Carbon and oxygen isotope values for abiotic aragonite, coral aragonite, and ferroan calcite at Ambitle Island (modified after Pichler and Dix, 1996). (a) Tutum Bay aragonite data only. (b) Comparison between Tutum Bay aragonite, ferroan calcite and other carbonates (modified after Pichler and Dix, 1996). Sources for other data are as follows: hermatypic corals (HC) (Tucker and Wright, 1990); low temperature aragonite (LTA), experimentally determined (Tarutani et al., 1969); aragonite (A) and Mg-calcite (MgC) cements (Gonzalez and Lohmann, 1985); and Lake Tanganyika hydrothermal aragonite (LTC) and Mg-calcite (Stoffers and Botz, 1994).

spots of the coarse aragonite (V-2(x)) by proton probe yielded the following average concentrations: Ca 360,0000 ppm, Sr 12,000 ppm, Fe 80 ppm and Mn 50 ppm, with little to none internal variation. In contrast, the analyses of 10 spots of the fine-grained aragonite (V-2(m)) showed lower Ca 340,0000 ppm and Sr 11,000 ppm and higher Fe 100 ppm and Mn 80 ppm, with little to none internal variation.

Rare earth element (REE) concentrations for hydrothermal aragonite, normalized to North American Shale Composite (NASC) (Haskin et al., 1968) are presented in Fig. 4. The patterns of samples V-2 and V-3 show an initial drop from La to Ce, followed by a rise from the Ce minimum to an Eu maximum and a constant decrease towards a Lu minimum. From La to Tb the pattern geometry closely resembles that of the parent hydrothermal fluid (Fig. 4a,b). The hydrothermal fluid pattern has a small increase in Dy before it decreases towards an intermediate Lu. The patterns for coarse and micro-crystalline aragonite in sample V-2 are effectively the same, except that the coarse aragonite shows significantly higher overall concentrations. The two samples from vent 4 are different and more closely resemble the pattern of the parent hydrothermal fluid (Fig. 4c). REE concentrations initially drop from La to a Ce minimum which is followed by a rise to a Eu (V-4.2) or Dy (V-4.1) maximum and a slight decrease towards Lu.

4.2. Isotopic composition

C and O isotope values of aragonite are plotted in Fig. 5. Collectively, $\delta^{18}O$ and $\delta^{13}C$ values are more negative than those expected for abiotic aragonite

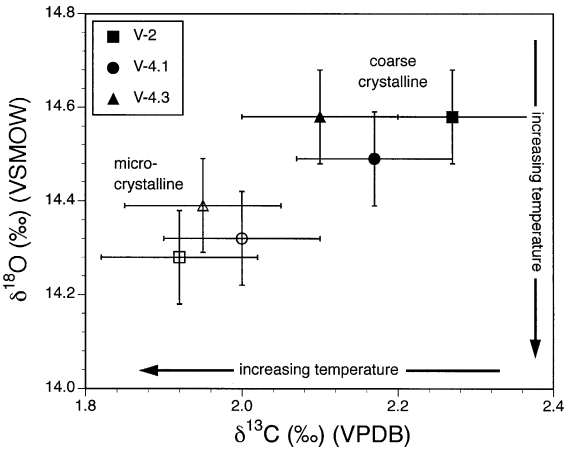

Fig. 6. $\delta^{13}C$ and $\delta^{18}O$ plot for micro crystalline and coarse crystalline aragonite. The arrows indicate the temperature trends for equilibrium precipitation. Based on equilibrium fractionation calculations (Friedman and O'Neil, 1977), the lower $\delta^{18}O$ and $\delta^{13}C$ values suggest precipitation at higher temperature.

Table 4
Isotopic composition of hydrothermal aragonite from Tutum Bay

Sample	$\delta^{18}O$ (VSMOW) ‰	$\delta^{18}O$ (PDB) ‰	$\delta^{13}C$ (PDB) ‰	$^{87}Sr/^{86}Sr \pm 2$ standard errors
V-2D	14.5	−15.8	2.2	0.704142 ± 13
V-2E	14.5	−15.8	2.0	n.d.
V-2D	14.6	−15.7	2.1	0.704097 ± 10
V-3A	14.5	−15.8	2.1	0.704097 ± 08
V-4.1A	14.4	−16.0	1.9	n.d.
V-4.2B	14.5	−15.8	2.1	n.d.
FV-3A[a]	14.9	−15.9	2.2	0.704149 ± 17
FV-4A[a]	14.6	−15.7	2.1	n.d.
FV-4B[a]	14.5	−15.8	2.0	n.d.
V-2(x)	14.5	−15.8	2.2	n.d.
V-2(m)	14.2	−16.1	1.9	n.d.
V-4.1(x)	14.4	−15.9	2.1	0.704131 ± 14
V-4.1(m)	14.3	−16.0	2.0	0.704551 ± 08
V-4.3(x)	14.5	−15.8	2.1	n.d.
V-4.3(m)	14.3	−16.0	1.9	n.d.

[a] Values are from Pichler and Dix (1996).

precipitated at low (25 °C) temperatures characteristic of shallow-water, tropical settings (Fig. 5b). $\delta^{13}C$ values, however, are within the ranges expected for marine carbon (Anderson and Arthur, 1983) and slightly higher than for abiotic aragonite from Lake Tanganyika that is interpreted to have incorporated hydrothermal CO_2 (Stoffers and Botz, 1994). The $\delta^{18}O$ value of a scleractinian coral, dead at the time of sampling, is distinct from the value of encrusting microcrystalline aragonite and falls just below the lower limit of the field defined by hermatypic corals (Fig. 5b).

A closer look at the samples that were collected by micro-drilling reveals that micro-crystalline and coarse-crystalline aragonite have a slightly different isotope signature. Micro-crystalline aragonite has lower $\delta^{18}O$ and $\delta^{13}C$ values (Fig. 6), but a higher $^{87}Sr/^{86}Sr$ (Table 4). Assuming isotopic equilibrium, the lower $\delta^{18}O$ and $\delta^{13}C$ values would indicate that the micro-crystalline aragonite precipitated either at higher temperatures or from a fluid with lower $\delta^{18}O$ and $\delta^{13}C$ values.

The $^{87}Sr/^{86}Sr$ values for hydrothermal aragonite (~ 0.7041) are almost identical to Tutum Bay vent fluids (Table 1) and to volcanic rocks collected on the island (M. Perfit, pers. comm.) (Fig. 7). They are also similar to values for submarine volcanic rocks that were dredged ~ 2 km southwest of Tutum Bay (Johnson et al., 1988). Bulk skeletal aragonite of a dead scleractinian coral that was collected immediately adjacent to vent 3, however, has a value interme-

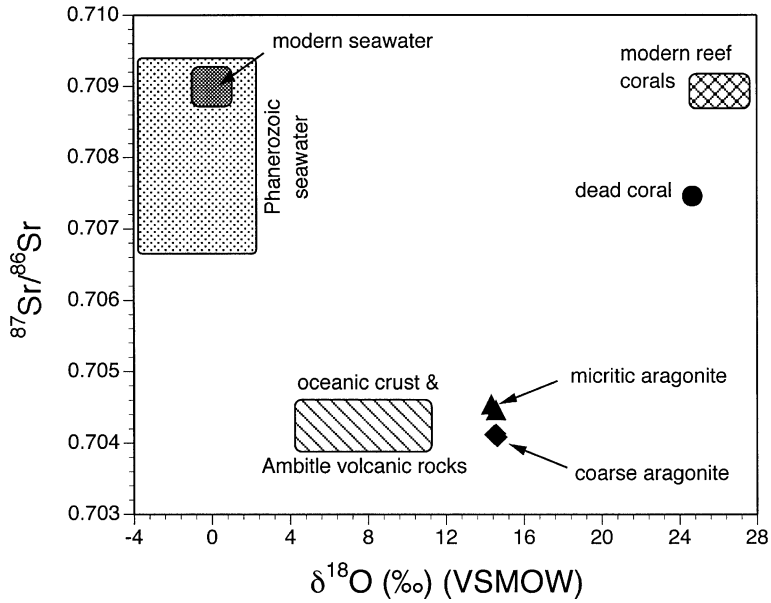

Fig. 7. $^{87}Sr/^{86}Sr$ ratios for hydrothermal and coral aragonite (modified after Pichler and Dix, 1996). Heavy stippled area is present-day seawater, and lighter stippled area is an approximate range of seawater compositions through Phanerozoic times. Sources for volcanic rock are from Hoefs (1997) and M. Perfit (pers. comm.).

diate between values of oceanic crust and modern seawater (Table 4 and Fig. 7). This intermediate $^{87}Sr/^{86}Sr$ value is caused by precipitation of hydrothermal aragonite in its skeleton after coral demise (Fig. 2b).

5. Discussion

The physico-chemical conditions of aragonite precipitation in Tutum Bay, although occurring submarine, are close to those of carbonate formation in terrestrial hot springs. The hydrothermal fluids are of meteoric origin and phase separation (degassing and boiling) is occurring within the vents (Pichler et al., 1999). Phase separation, however, ceases immediately above the vent orifices due to mixing with ambient seawater and thus rapid cooling. Given the shallow depth in Tutum Bay (6–9 m), ambient pressure is not dramatically different from on-land settings; 1.6 to 1.9 atm vs. 1 atm The physico-chemical conditions in deep sea hydrothermal systems, on the other hand, are drastically different. There, hydrothermal fluids are of seawater origin and due to the enormous water pressure, boiling is only rarely observed (Von Damm, 1995). The concentration of sulfide is high and the amount of dissolved carbonate is relatively low, thus the formation of carbonate minerals is, if not completely absent, secondary to the precipitation of sulfides and sulfates (Alt, 1995; Rona, 1984; Von Damm, 1990, 1995).

The precipitation of a carbonate phase from solution is primarily controlled by pCO_2, pH, temperature, ion activity and microbial activity (e.g., Ford and Pedley, 1996). These factors are closely related and they often compete with each other. The formation of travertine deposits in CO_2-rich springs, for example, is a result of CO_2 degassing due to a drop in pressure (e.g., Jones and Renaut, 1996; Pentecost, 1995; Renaut and Jones, 1997). At the same time, however, cooling of the spring water may increase carbonate solubility and whether precipitation takes place is determined by the respective intensity of these competing processes. Hydrothermal fluids in Tutum Bay are CO_2-rich (pCO_2>2 atm), boiling or close to boiling as they enter seawater (Pichler and Dix, 1996); this causes a rapid loss of CO_2. Mixing of the Tutum Bay hydrothermal fluids with seawater would cause a drop in temperature and an increase in pH, the latter favoring carbonate precipitation. To further investigate the precipitation process, it is necessary to determine if there is mixing between hydrothermal fluid and seawater and to assess its magnitude prior to and during precipitation.

$^{87}Sr/^{86}Sr$ ratios are a widely used tracer in mixing processes (Faure, 1986). The mass difference between the two strontium isotopes, ^{87}Sr and ^{86}Sr, is too small to cause a measurable fractionation during precipitation. Thus the $^{87}Sr/^{86}Sr$ ratio in aragonite can be used as a direct measure of its ratio in the parent fluid. $^{87}Sr/^{86}Sr$ values in hydrothermal aragonite indicate that some mixing with seawater occurs during its precipitation (Fig. 8). Neglecting a difference in heat

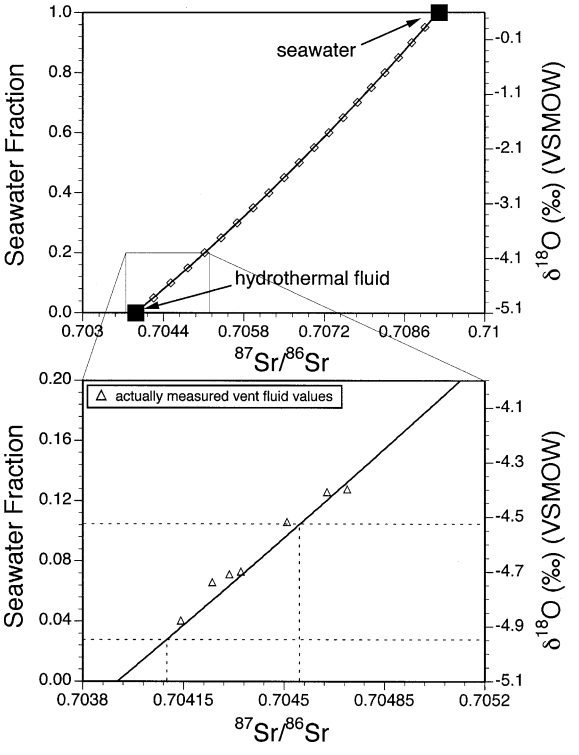

Fig. 8. Mixing curve between the hydrothermal fluid and seawater based on Sr concentration, $^{87}Sr/^{86}Sr$ ratios and $\delta^{18}O$ values. The curve was calculated following Faure (1986). The open triangles represent actually measured $^{87}Sr/^{86}Sr$ and $\delta^{18}O$ values in Tutum Bay hydrothermal fluids (Pichler, 1998, 2003). Dashed lines indicate the range of $^{87}Sr/^{86}Sr$ in Tutum Bay aragonite and the corresponding $\delta^{18}O$ and seawater fraction.

capacity and assuming seawater and hydrothermal fluid to be 30 and 100 °C, respectively, the temperature of the mixture can be calculated with the mass balance equation:

$$t_M = (1-y)t_{HF} + yt_{SW} \quad (1)$$

where t is the temperature in °C, y is the seawater fraction and the subscripts M, HF and SW indicate the final mixture, the hydrothermal fluid and seawater, respectively. The calculated maximum seawater fraction, using the Sr-data for aragonite, is 11% (Fig. 8), which corresponds to a maximum temperature drop by approximately 7 to 93 °C. The corresponding maximum change in pH is about 0.2 units. The calculated extent of mixing, although very small, may prevent precipitation if one of the mixing partners is dramatically undersaturated with respect to calcium carbonate. In Tutum Bay, however, both seawater and hydrothermal fluid are supersaturated with respect to calcium carbonate and the relatively elevated activity of Ca^{2+} in seawater may actually be the trigger that initiates nucleation (Dandurand et al., 1982).

Microbial activity can greatly enhance the precipitation of carbonates in warm-springs ($t < 70$ °C) (e.g., Folk, 1994), but the temperatures of Tutum Bay vents are possibly too high to allow for extensive microbial activity and precipitation should therefore be controlled mainly by inorganic factors.

Of the factors that control precipitation in most on-land hot-springs and in Tutum Bay, CO_2 degassing is arguably the single most important (e.g., Dandurand et al., 1982; Renaut and Jones, 1997; Simmons and Christenson, 1994; Usdowski et al., 1979). CO_2 degassing increases the pH and subsequently increases supersaturation, leading to the precipitation of calcium carbonate:

$$Ca^{2+} + 2HCO_3^- \Rightarrow CaCO_3 + H_2O + CO_2\uparrow . \quad (2)$$

The hydrothermally precipitated carbonate mineral in Tutum Bay is completely in the form of aragonite, which is surprising considering that the parent hydrothermal fluid is slightly more supersaturated with respect to calcite ($SI_{cacite} = 0.65$ and $SI_{aragonite} = 0.55$). The formation of either aragonite or calcite is still poorly understood, but it is clear that no single fluid parameter is likely to be the sole or dominant control in natural environments (Burton, 1993).

Precipitation of aragonite rather than calcite is a common process in tropical shallow-water submarine environments (Tucker and Wright, 1990). In hydrothermal systems, however, calcite is the primary carbonate precipitate, and the presence of aragonite is usually attributed to rapid precipitation rates, elevated Mg/Ca, and stabilizing effects of Ba, Sr and possibly Mg on the orthorhombic crystal structure (Browne, 1973; Folk, 1994). Folk (1994) suggested that aragonite is the preferential precipitate relative to calcite in hot springs at temperatures >40 °C or with a mMg/mCa of >1 at temperatures below 40 °C. Mg/Ca ratios in Tutum Bay vent fluids are rather low, but temperatures are >40 °C and precipitation rates, although unknown, should be high considering the amount of CO_2 released. The alternation between aragonite and calcite in hot spring travertine at Lake Bogoria, Kenya (Renaut and Jones, 1997), for example, has been attributed to pCO_2 and precipitation rate. There, Mg/Ca ratios are also low, but precipitation of aragonite is favored under conditions of high pCO_2 and rapid precipitation. The change in mineralogy at Lake Bogoria is accompanied by a change in crystal habit and size (Fig. 5 in Renaut and Jones, 1997) from coarse crystalline aragonite to fine grained calcite (feather dendrite). The same change in crystal habit and size can be observed in Tutum Bay aragonite (Fig. 3), but without any change in mineralogy. Relatively higher $^{87}Sr/^{86}Sr$ ratios in the fine-grained aragonite (Fig. 7 and Table 4) should indicate a larger presence of seawater during crystal precipitation and growth. Addition of seawater to the hydrothermal fluid causes a change in super-saturation, which in turn may affect the crystal habit; thus the change from coarse to fine-grained aragonite. It is noteworthy however, that the $\delta^{18}O$ and $\delta^{13}C$ equilibrium temperatures are slightly higher for the fine-grained aragonite than those for the bigger crystals (Fig. 6), an observation at odds with the advocated higher seawater fraction. This enigma is explained below.

The generally low trace element concentrations in hydrothermal aragonite are as expected for orthorhombic carbonates (Speer, 1983; Veizer, 1983). This is a result of their low distribution coefficients and low concentrations in the hydrothermal fluid (Pichler et al., 1999). Among the processes that directly

incorporate minor and trace elements into orthorhombic carbonate minerals, substitution for Ca in the $CaCO_3$ structure is the most important. Incorporation is generally limited by the charge and size of the metal cation and, therefore, aragonite preferentially incorporates divalent cations larger than Ca (Speer, 1983). Despite their higher charge of 3+ vs. 2+ for Ca and with exception of Eu^{2+}, the rare earth elements (REEs) in Tutum Bay hydrothermal aragonite are highly concentrated relative to the vent fluid (Fig. 4). The REE patterns for samples V-2 and V-3 clearly demonstrate the importance of the ionic radius for substitution. The concentrations of REEs with ionic radii larger than or similar to Ca (La to Tb) seem to be controlled by their concentration in the hydrothermal fluid, while those with ionic radii smaller than Ca (Dy to Lu) are relatively depleted (Fig. 4a,b). The difference in pattern geometry between the samples from vents 2 and 3 and those from vent 4, V-4.1 and V-4.2 (Fig. 4c) is the result of the slightly different REE composition of vent 4 (Table 3).

The obvious difference in concentration and pattern geometry between the coarse crystalline (V-2(x)) and fine crystalline aragonite (V-2(m)) (Fig. 4a) is probably a result of seawater mixing during precipitation (see above). The addition of small amounts of seawater may be sufficient for the formation of a variety of REE complexes, such as $LaCl^{2+}$, $LaCO_3^+$and $LaSO_4^+$, which affect their availability for substitution of Ca, resulting in lower total concentrations and in a flatter slope between Eu and Lu. In particular, a change in precipitation and growth rate may account for the different patterns and concentrations of V-2(m) and V-2(x) (Fig. 4a).

5.1. Isotopic equilibrium—yes or no?

Attainment of isotopic equilibrium between a hydrothermal precipitate and its parent solution is a prerequisite to the application of any isotope geothermometer when absolute rather than relative temperatures are to be calculated. The reconstruction of physico-chemical conditions in fossil hydrothermal systems can be aided by analyses of $\delta^{18}O$ and $\delta^{13}C$ in carbonate minerals (e.g., Ohmoto and Rye, 1979; Simmons and Christenson, 1994), although the existence of isotopic equilibrium is uncertain. Modern hot spring travertines provide natural laboratories to study isotope systematics and to assess equilibrium conditions. Several studies (e.g., Amundson and Kelly, 1987; Dandurand et al., 1982) found that carbonates were not in oxygen-isotope equilibrium with the parental waters, while at the same time carbon-isotope equilibrium was attained.

Tutum Bay provides an exceptional location for the study of mineral precipitation and the evaluation of equilibrium conditions. Conditions here are almost as controlled as in a laboratory. Five visits to Tutum Bay have provided us with a time series of field observations and chemical and isotopic data, indicating the physicochemical stability of the Tutum Bay hydrothermal system. The chemical and isotopic composition of the vent fluids has remained stable since our first sampling in 1994; oxygen isotope values, for example, did not vary beyond their analytical error of approximately 0.1‰ to 0.2‰ (Pichler, 1998). This is also demonstrated by the uniform oxygen and carbon isotopic compositions of the aragonite samples (Table 4).

In the absence of any fractionation factor for abiotic aragonite at temperatures above 40 °C, the calcite–water fractionation factor from Friedman and O'Neil (1977) was used because the differences between these two fractionation factors appear to be insignificant above 30 °C (Anderson and Arthur, 1983). Following Friedman and O'Neil (1977), and assuming isotopic equilibrium, an average aragonite precipitation temperature of approximately 78 °C was calculated, using the mean $\delta^{18}O$ of aragonite (14.5‰) and that of the hydrothermal fluid (−5.1‰; from Pichler, 1998). The possible range of equilibrium temperatures using all $\delta^{18}O$ values of aragonite and vent fluids is shown in Fig. 9 (Area A). These temperatures are lower than those estimated from $^{87}Sr/^{86}Sr$ mixing calculations by about 18 °C (Fig. 9, Area C). Based on $^{87}Sr/^{86}Sr$ mixing calculations, the amount of seawater present during precipitation of aragonite ranged from approximately 3% to 11% (Fig. 8). Assuming seawater and hydrothermal fluid to be 30 and 100 °C, respectively, the temperature of the mixtures and, hence, the possible range of precipitation temperatures can be calculated. These calculated temperatures range from 92.3 to 97.9 °C would correspond to an equilibrium $\delta^{18}O$ of approximately −3‰ in the hydrothermal fluid. This value is in

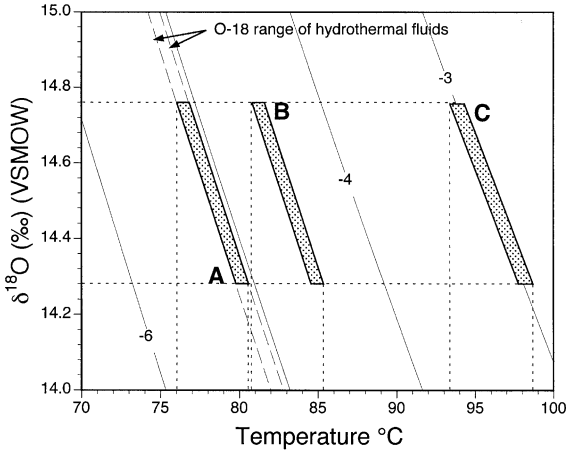

Fig. 9. Plot of $\delta^{18}O$ equilibrium temperatures in the system calcite–H_2O. The curves (solid lines) represent the calculated isotopic composition of calcite in equilibrium with water of −3‰, −4‰, −5‰ and −6‰ as a function of temperature using the equation from Friedman and O'Neil (1977). The dashed curves represent the range of $\delta^{18}O$ in Tutum Bay vent waters. Area A represents the possible range of isotopic equilibrium for Tutum Bay hydrothermal aragonite. Area B represents the possible range of isotopic equilibrium for the maximum seawater component during precipitation (see the text for more explanation). Area C represents the expected range of isotopic equilibrium and $\delta^{18}O$ of the hydrothermal fluid based on temperatures derived from mixing considerations for $^{87}Sr/^{86}Sr$ (see text).

disagreement with the measured hydrothermal fluid $\delta^{18}O$ of −5.1‰ (Pichler, 1998).

Some of the discrepancy between the $\delta^{18}O$ and the $^{87}Sr/^{86}Sr$ precipitation temperatures can be explained by the inverse effect of seawater mixing. On one hand, mixing with ambient seawater cools the hydrothermal fluid, while on the other, addition of seawater-derived ^{18}O leads to the calculation of higher precipitation temperatures for the same $\delta^{18}O$ value for aragonite (Fig. 9, Areas B and C). For example, aragonite with a $\delta^{18}O$ of 14‰ is in equilibrium with water of −6‰ and −4‰ at ~75 and ~91.5 °C, respectively (Fig. 9). If the maximum amount of seawater is added, the $\delta^{18}O$ of the hydrothermal fluid increases to approximately −4.5‰ (Fig. 8), which results in precipitation temperatures between 80.5 and 85 °C (Fig. 9, Area B). This temperature range, although higher than the pre-mixing $\delta^{18}O$ equilibrium temperatures, is still low when compared to the $^{87}Sr/^{86}Sr$ mixing temperatures (Fig. 9, Area C).

The $\delta^{13}C$ calcite–CO_2 geothermometer has been successfully applied in many studies of hydrothermal ore deposits and temperatures of precipitation can be determined within ±20 °C (Ohmoto and Rye, 1979). The calcite–CO_2 geothermometer has the advantage that mixing with ambient seawater can be neglected due to the immense concentration difference. Equilibrium temperatures were evaluated using two different data sets, (1) the theoretical computations by Bottinga (1968) and (2) those by Chacko et al. (1991). At high temperature (>300 °C) both data sets are in good agreement, but below 300 °C their fractionation factors become increasingly different with decreasing temperature (Figs. 10 and 5 in Chacko et al., 1991). Equilibrium precipitation temperatures for the $\delta^{13}C$ range of Tutum Bay CO_2 gas (−2.5‰ to −2.2‰; from Pichler, 1998, 2003) are 82 to 91 °C and 87.5 to 98 °C for the fractionation factors from Chacko et al. (1991) and Bottinga (1968), respectively (Fig. 10). Both temperature ranges are larger than those based on $\delta^{18}O$ values of the aragonite samples, but they are in better agreement with the $^{87}Sr/^{86}Sr$ mixing temperatures. The $\delta^{13}C$ temperatures calculated with the fractionation factors from Bottinga (1968) cover the temperature range obtained from $^{87}Sr/^{86}Sr$ mixing calculations (Fig. 10a), while those using the fractionation factors from Chacko et al. (1991) are lower but closer to the $\delta^{18}O$ temperatures (Fig. 10b).

Seawater mixing during precipitation may explain the apparent increase in temperature between coarse and micro-crystalline aragonite (Fig. 6). Precipitation rate is not a factor because it has no influence on the oxygen isotopic composition of purely inorganic carbonates (Kim and O'Niel, 1997; Tarutani et al., 1969). The difference in $\delta^{13}C$ on the other hand may be caused by a change in precipitation rate. Romanek et al. (1992) noted a small positive relationship between precipitation rate and fractionation factor at 40 °C.

The temperatures obtained from isotope geothermometry are in good agreement with those from fluid inclusions (80 to 110 °C) and those measured in the field (94 to 98 °C) (Pichler and Dix, 1996). Similar to observations from onland hot springs (e.g., Amundson and Kelly, 1987; Dandurand et al., 1982), it seems that in Tutum Bay the aragonite precipitated in $\delta^{13}C$ equilibrium with CO_2, while

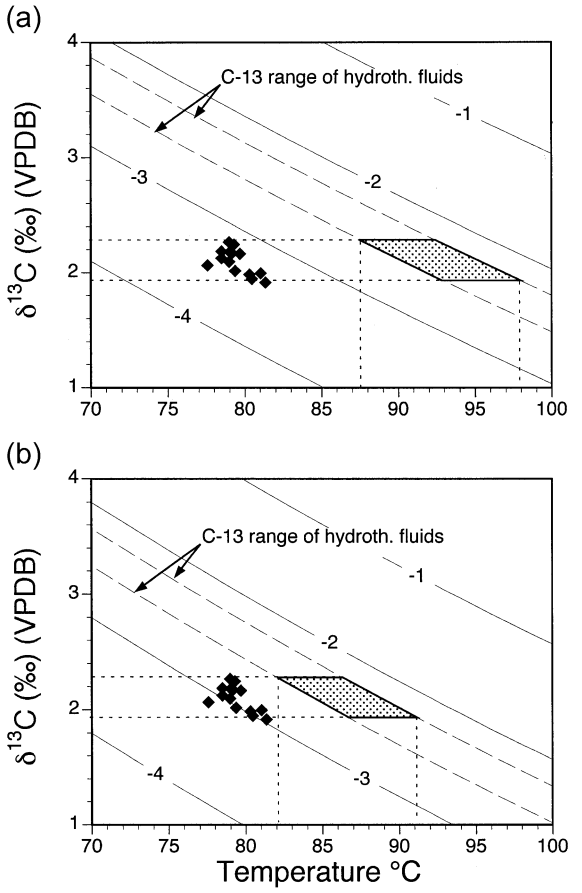

Fig. 10. Plot of $\delta^{13}C$ equilibrium temperatures in the system calcite–CO_2 (a) based on data from Bottinga (1968) and (b) based on data from Chacko et al. (1991). The curves (solid lines) represent the calculated isotopic composition of calcite in equilibrium with CO_2 of −1‰, −2‰, −3‰ and −4 ‰ as a function of temperature. Diamonds represent calculated $\delta^{18}O$ equilibrium temperatures.

$\delta^{18}O$ equilibrium with water was apparently not attained. However, once the aragonite forming source water is assumed to be a mixture of a hydrothermal and seawater endmember with a $\delta^{18}O$ of −4.5‰, the difference between minimum and maximum precipitation temperature is less than 10 °C. This difference in calculated equilibrium temperature is surprisingly small considering the difficulties associated with obtaining accurate isotope fractionation factors under laboratory conditions (e.g., Chacko et al., 1991; Kim and O'Niel, 1997; Romanek et al., 1992).

6. Summary and conclusions

Tutum Bay hydrothermal vent waters are actively depositing substantial amounts of aragonite as massive layers of euhedral, pseudo-hexagonal crystals up to 2 cm long and as micro-crystalline aragonite. Pseudo-hexagonal crystals are often terminated by micro-crystalline crystals that mimic feather dendrites (Fig. 3). Near vent sites, primary pore space in volcaniclastic sediment and in skeletons of dead corals is almost completely occluded by hydrothermal aragonite.

Hydrothermal aragonite has a distinctively different isotopic composition when compared to "normal" shallow-water marine carbonate. This difference arises from precipitation at high temperature from a mixture of seawater and hydrothermal fluid that has lower $^{87}Sr/^{86}Sr$ (approximately 0.704) and $\delta^{18}O$ (−4.5‰ VSMOW) values than seawater (0.709‰ and 0‰ VSMOW). Based on $^{87}Sr/^{86}Sr$ mixing calculations, the maximum seawater fraction is approximately 11%. Apparently, carbon isotopic equilibrium has been reached, while for oxygen complete equilibrium was not attained. Calculated equilibrium temperatures (78 °C), nevertheless, are close to those directly measured (89–98 °C) and those obtained from fluid inclusion experiments (80–110 °C) (Pichler and Dix, 1996).

An alternative explanation for the discrepancy between the measured and calculated could be that the assumption of identical fractionation factors for aragonite and calcite at higher temperatures is not correct. Assuming that the aragonite in Tutum Bay precipitated in equilibrium with its parent fluid, the data presented here can be used for a $\delta^{18}O$ aragonite–water fractionation factor at 100 °C.

The $^{87}Sr/^{86}Sr$ composition of Tutum Bay aragonite, primarily controlled by hydrothermal strontium, is dramatically different from recent marine carbonates, which precipitate from seawater. This has implications for marine carbonates that may have accumulated in a similar environment, if the time-dependent variations of $^{87}Sr/^{86}Sr$ ratios (e.g., Burke et al., 1982; Veizer, 1989) were utilized for dating. According to its $^{87}Sr/^{86}Sr$ ratio, the aragonite from Tutum Bay would have an improbable Late Cretaceous age.

Trace element concentrations of aragonite, except for the REEs, Y and Sr are low. The REE pattern

geometry of aragonite is similar to that of the hydrothermal fluid and concentrations are higher in coarse aragonite than in fine-grained examples. This may be caused by higher precipitation rates.

Acknowledgements

Most of this research was funded by an American Chemical Society, Petroleum Research Grant (No. 31585-AC8) and Natural Sciences and Engineering Research Council of Canada operating grant to Jan Veizer. We are grateful to Donna Switzer and Yannick Beaudoin for help underwater, to Dieter Buhl for the strontium isotope analyses, to Frank Bruhn for the PIXE analyses and to Philip Tolain and all the friendly people of Ambitle Island for their hospitality. Thanks to Wolfgang Bach, Ian Clark and Robert Folk for comments on an earlier version. The final version benefited greatly from two excellent reviews by Rainer Botz and Jens Greinert. **[LW]**

References

Alt, J.C., 1995. Subseafloor processes in mid-ocean ridge hydrothermal systems. In: Humphries, S.E., Zierenberg, R.A., Mullineaux, L.S., Thomson, R.E. (Eds.), Seafloor Hydrothermal Systems. Volume Geophysical Monograph 91. American Geophysical Union, pp. 85–114.

Amundson, R.G., Kelly, E., 1987. The chemistry and mineralogy of a CO_2 -rich travertine depositing spring in the California Coast Range. Geochim. Cosmochim. Acta 51 (11), 2883–2890.

Anderson, T.F., Arthur, M.A., 1983. Stable isotopes of oxygen and carbon and their application to sedimentologic and paleoenvironmental problems. In: Arthur, M.A., Anderson, T.F., Kaplan, I.R., Veizer, J., Land, L.S. (Eds.), Stable Isotopes in Sedimentary Geology. SEPM Short Course, 1–151. Columbia, SC.

Bottinga, Y., 1968. Calculation of fractionation factors for carbon and oxygen isotopic exchange in the system calcite–carbon dioxide–water. J. Phys. Chem. 72, 800–808.

Browne, P.R.L., 1973. Aragonite deposited from broadlands geothermal drillhole water. N.Z. J. Geol. Geophys. 16 (4), 927–933.

Bruhn, F., et al., 1995. Diagenetic history of sedimentary carbonates: constraints from combined cathodoluminescence and trace element analyses by micro-PIXE. Nucl. Instrum. Methods 104, 409–414.

Buhl, D., et al., 1991. Nature and nurture: environmental isotope story of the river Rhine. Naturwissenschaften 78, 337–346.

Burke, W.H., et al., 1982. Variation of seawater $^{87}Sr/^{86}Sr$ throughout Phanerozoic time. Geology 10, 516–519.

Burton, E.A., 1993. Controls on marine carbonate cement mineralogy: review and reassessment. Chem. Geol. 105, 163–179.

Chacko, T., Mayeda, T.K., Clayton, R.N., Goldsmith, J.R., 1991. Oxygen and carbon isotope fractionations between CO_2 and calcite. Geochim. Cosmochim. Acta 55 (10), 2867–2882.

Dandurand, J.L., et al., 1982. Kinetically controlled variations of major components and carbon and oxygen isotopes in a calcite-precipitating spring. Chem. Geol. 36, 299–315.

Desrochers, A., Al-Aasm, I.S., 1993. The formation of septarian concretions in Queen Charlotte Islands, B.C.: evidence for microbially and hydrothermally mediated reactions at shallow burial depth. J. Sediment. Petrol. 63 (2), 282–294.

Diener, A., Ebneth, S., Veizer, J., Buhl, D., 1996. Strontium isotope stratigraphy of the Middle Devonian: brachiopods and conodonts. Geochim. Cosmochim. Acta 60, 639–652.

Faure, G., 1986. Principles of Isotope Geochemistry. Wiley, New York. 589 pp.

Folk, R.L., 1994. Interaction between bacteria, nannobacteria, and mineral precipitation in hot springs of central Italy. Géogr. Phys. Quat. 48 (3), 233–246.

Ford, T.D., Pedley, H.M., 1996. A review of tufa and travertine deposits of the world. Earth-Sci. Rev. 41, 117–175.

Friedman, I., O'Neil, J.R. (Eds.), 1977. Compilation of Stable Isotope Fractionation Factors of Geochemical Interest. Data of Geochemistry. U.S. Geological Survey Professional Paper, vol. 440-KK. Washington, 12 pp.

Gonzalez, L.A., Lohmann, K.C., 1985. Carbon and oxygen isotopic composition of Holocene reefal carbonates. Geology 13, 811–814.

Hall, G.E.M., 1992. Inductively coupled plasma mass spectrometry in geoanalysis. Journal of Geochemical Exploration 44, 201–249.

Haskin, L.A., Haskin, M.A., Frey, F.A., Wildman, T.R., 1968. Relative and absolute terrestrial abundance of the rare earths. In: Ahrens, L.H. (Ed.), Origin and Distribution of the Elements. Pergamon, Oxford, pp. 889–911.

Hoefs, J., 1997. Stable Isotope Geochemistry. Springer, Berlin, p. 202.

Hovland, M., 1990. Do carbonate reefs form due to fluid seepage? Terra Nova 2, 8–18.

Johnson, R.W., et al., 1988. Volcanism in the New Ireland basin and Manus island region: notes on the geochemistry and petrology of some dredged volcanic rocks from a rifted-arc region. In: Marlow, M.S., Dadisman, S.V., Exon, N.F. (Eds.), Geology and offshore resources of Pacific island arcs—New Ireland and Manus region, Papua New Guinea. Circum-Pacific Council for Energy and Mineral Resources, Houston, pp. 113–130.

Jones, B., Renaut, R.W., 1996. Morphology and growth of aragonite crystals in hot-spring travertines at Lake Bogoria, Kenya Rift Valley. Sedimentology 43 (2), 323–340.

Kaufmann, B., Wendt, J., 2000. Calcite cement successions in Middle Devonian (Givetian) carbonate mud buildups of the southern Ahnet Basin (Algerian Sahara). Carbonates Evaporites 15 (2), 149–161.

Kaufman, E.G., Arthur, M.A., Howe, B., Scholle, P.A., 1996. Widespread venting of methane-rich fluids in Late Cretaceous (Cam-

panian) submarine springs (Tepee Buttes), Western Interior seaway, USA. Geology 24, 799–802.

Kim, S.-T., O'Niel, J.R., 1997. Equilbrium and nonequilibrium oxygen isotope effects in synthetic carbonates. Geochim. Cosmochim. Acta 61 (16), 3461–3475.

Licence, P.S., Terrill, J.E., Fergusson, L.J., 1987. Epithermal gold mineralization, Ambitle Island, Papua New Guinea, Pacific Rim Congress 87. Australasian Institute of Mining and Metallurgy, Gold Coast, Queensland, pp. 273–278.

Maxwell, J.A., Teesdale, W.J., Campbell, J.L., 1995. The Guelph PIXE software package II. Nucl. Instrum. Methods Phys. Res. B95, 407–421.

Ohmoto, H., Rye, R.O., 1979. Isotopes of sulfur and carbon. In: Barnes, H.L. (Ed.), Geochemistry Hydrothermal Ore Deposits. Wiley, New York, pp. 509–567.

Pentecost, A., 1995. Geochemistry of carbon dioxide in six travertine-depositing waters of Italy. J. Hydrol. 167, 263–278.

Pichler, T., 1998. Shallow-water hydrothermal activity in a coral-reef ecosystem, Ambitle Island, Papua New Guinea. PhD thesis, University of Ottawa, Ottawa, 206 pp.

Pichler, T., Dix, G.R., 1996. Hydrothermal venting within a coral reef ecosystem, Ambitle Island, Papua New Guinea. Geology 20 (5), 435–438.

Pichler, T., Veizer, J., Hall, G.E.M., 1999. The chemical composition of shallow-water hydrothermal fluids in Tutum Bay, Ambitle Island, Papua New Guinea and their effect on ambient seawater. Mar. Chem. 64 (3), 229–252.

Pichler, T., Heikoop, J., Risk, M., Veizer, J., Campbell, I., 2000. Hydrothermal effects on isotope and trace element records in modern reef corals: an introductory study of Porites lobata from Tutum Bay, Ambitle Island, Papua New Guinea. Palaios 15 (3), 225–234.

Renaut, R.W., Jones, B., 1997. Controls on aragonte and calcite precipitation in hot spring travertines at Chemurkeu, Lake Bogoria, Kenya. Can. J. Earth Sci. 34, 801–818.

Romanek, C.S., Grossman, E.L., Morse, J.W., 1992. Carbon isotopic fractionation in synthetic aragonite and calcite: effects of temperature and precipitation rate. Geochim. Cosmochim. Acta 56 (1), 419–430.

Rona, P.A., 1984. Hydrothermal mineralization at seafloor spreading centers. Earth-Sci. Rev. 20, 1–104.

Simmons, S.F., Christenson, B.W., 1994. Origins of calcite in a boiling geothermal system. Am. J. Sci. 294, 361–400.

Speer, J.A., 1983. Crystal chemistry and phase relations of orthorhombic carbonates. In: Reeder, R.J. (Ed.), Carbonates: Mineralogy and Chemistry. Reviews in Mineralogy Mineralogical Society of America, Washington, pp. 145–189.

Stoffers, P., Botz, R., 1994. Formation of hydothermal carbonate in Lake Tanganyika, East-Central Africa. Chem. Geol. 115, 117–122.

Switzer, D.G., 1997. Recent benthic foraminifera in a shallow hydrothermally vented patch reef off Ambitle Island, Papua New Guinea. BSc Honors Thesis, Carleton University, Ottawa, 97 pp.

Tarutani, T., Clayton, R.N., Mayeda, T.K., 1969. The effect of polymorphism and magnesium substitution on oxygen isotope fractionation between calcium carbonate and water. Geochim. Cosmochim. Acta 33, 987–996.

Tucker, M.E., Wright, V.P., 1990. Carbonate Sedimentology Blackwell, Oxford. 483 pp.

Usdowski, E., Hoefs, J., Menschel, G., 1979. Relationship between ^{13}C and ^{18}O fractionation and changes in major element composition in a recent calcite-depositing spring—a model of chemical variations with inorganic $CaCO_3$ precipitation. Earth Planet. Sci. Lett. 42, 267–276.

Veizer, J., 1983. Chemical diagenesis of carbonate rocks: theory and application of trace element technique. In: Arthur, M.A., Anderson, T.F. (Eds.), Stable Isotopes in Sedimentary Geology. Volume Short Course No. 10. Society of Economic Paleontologists and Mineralogists, Saskatoon, pp. 3.1–3.100.

Veizer, J., 1989. Strontium isotopes in seawater through time. Annu. Rev. Earth Planet. Sci. Lett. 17, 141–167.

Von Damm, K.L., 1990. Seafloor hydrothermal activity: black smoker chemistry and chimneys. Annu. Rev. Earth Planet. Sci. 18, 173–204.

Von Damm, K.L., 1995. Controls on the chemistry and temporal variability of seafloor hydrothermal systems. In: Humphries, S.E., Zierenberg, R.A., Mullineaux, L.S., Thomson, R.E. (Eds.), Seafloor Hydrothermal Systems, Volume Geophysical Monograph 91. American Geophysical Union, pp. 222–247.

Wallace, D.A., et al., 1983. Cainozoic volcanism of the Tabar, Lihir, Tanga, and Feni islands, Papua New Guinea: Geology, Whole-rock Analyses, and Rock-forming Mineral Compositions, vol. 243. Bureau of Mineral Resources Geology and Geophysics, Sydney.